

INTERPRETING THE PROPER MOTIONS OF THE HH 34S BOWSHOCK

A. C. Raga,¹ P. F. Velázquez,¹ J. Cantó,² and E. Masciadri²

Received 2002 April 17; accepted 2002 September 9

RESUMEN

Reipurth et al. (2002) han obtenido movimientos propios muy detallados del choque a proa HH 34S usando imágenes obtenidas con el *Hubble Space Telescope* (*HST*). Encontramos que estos movimientos propios pueden ser usados para reconstruir la velocidad de choque y la velocidad más allá de HH 34S en función de posición. De este ejercicio, obtenemos velocidades de choque en el intervalo de 60 a 120 km s⁻¹, lo cual concuerda con determinaciones previas basadas en el análisis de cocientes y perfiles de líneas de emisión. También deducimos la presencia de un flujo con velocidades de ≈ 200 km s⁻¹ más allá de HH 34S, el cual se extiende hasta $\sim 10''$ a cada lado del eje del sistema. Interpretamos este flujo como la estela dejada por eventos de eyección previos, y mostramos que una simulación numérica de una eyección con dependencia temporal logra reproducir las propiedades de este flujo en una forma convincente.

ABSTRACT

Reipurth et al. (2002) have obtained very detailed proper motions of the HH 34S bowshock using *Hubble Space Telescope* (*HST*) images. We find that these proper motions can be used to reconstruct the position-dependent shock velocity and the flow velocity ahead of the bowshock. From this exercise, we obtain shock velocities in the 60 to 120 km s⁻¹ range, in qualitative agreement with previous determinations based on the analysis of line profiles and line ratios. We also deduce the presence of a ≈ 200 km s⁻¹ flow directly ahead of HH 34S, extending out to $\sim 10''$ on each side of the outflow axis. We interpret this flow as the wake left behind by previous outflow events, and show that a variable ejection velocity gasdynamic jet simulation does reproduce the properties of this flow in a convincing way.

Key Words: HYDRODYNAMICS — ISM: INDIVIDUAL (HH 34) — ISM: JETS AND OUTFLOWS — STARS: PRE-MAIN-SEQUENCE

1. INTRODUCTION

Reipurth et al. (2002) have obtained new proper motions of the HH 34 system from high spatial resolution *Hubble Space Telescope* (*HST*) observations. These proper motions represent a clear improvement on previous proper motion measurements of this object obtained from ground based images (Heathcote & Reipurth 1992; Eisloffel & Mundt 1992). The only comparably detailed proper motion measurements of any HH object are the ones of HH 32 obtained by Curiel et al. (1997, who used *HST* and

ground based, adaptive optics images) and the ones of HH 1/2 obtained by Hartigan et al. (2001, from *HST* images).

The H α *HST* images show that HH 34S has a number of well defined, gently curved filaments that apparently correspond to segments of a fragmented bowshock. Reipurth et al. (2002) have measured the motions of many of these filaments. Interestingly, the proper motion vectors determined for these filaments deviate from the direction normal to the shock, systematically being directed in between the shock normal and the outflow axis. This effect is clearly visible in Figure 9 of Reipurth et al. (2002).

As shocks only push material in the direction parallel to the shock normal, the lack of alignment of

¹Instituto de Ciencias Nucleares, Universidad Nacional Autónoma de México.

²Instituto de Astronomía, Universidad Nacional Autónoma de México.

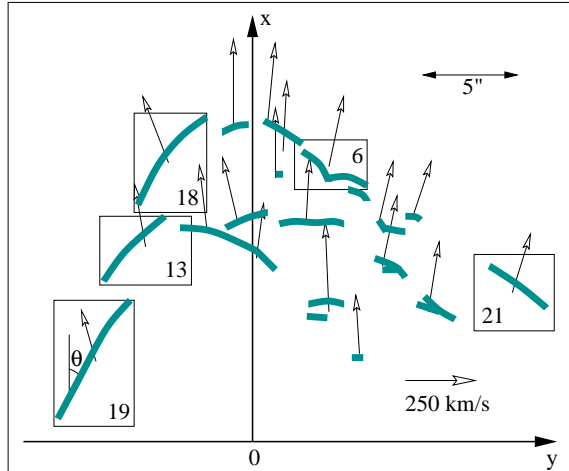


Fig. 1. Schematic diagram showing the filamentary structure observed in $H\alpha$ *HST* images of HH 34S and the proper motions derived by Reipurth et al. (2002). The x -axis approximately coincides with the outflow axis. We have chosen 5 of the cross-correlation boxes of Reipurth et al. (2002), which lie along the edge of the bowshock and which include filamentary structures with well defined orientations (the boxes are numbered 6, 13, 18, 19, and 21). The angle θ between the filaments and the outflow axis is defined as having a positive value, regardless of the orientation of the filaments.

the proper motions with the shock normal has two possible interpretations:

1. that the post-bowshock gas rapidly mixes with material from the jet, therefore acquiring momentum directed along the outflow axis,
2. that the component of the proper motion velocity directed parallel to the shock is already present in the pre-shock material.

As the HH 34S filaments do not appear to be corrugated in small scales, we feel that there is no direct observational evidence of the occurrence of strong turbulent mixing. Therefore, we feel that the second of the above possibilities appears to be more reasonable.

In § 2, we discuss the HH 34S proper motions of Reipurth et al. (2002), and present simple, analytic arguments from which the spatially resolved motion of the pre-bowshock gas can be obtained. In § 3 we discuss the possibility that this moving gas is the wake left behind by previous outflow episodes, and explore this scenario with an axisymmetric gasdynamic simulation. Finally, the results are summarized in § 4.

We should note that the analysis presented in § 2 is based on the implicit assumption that the observed

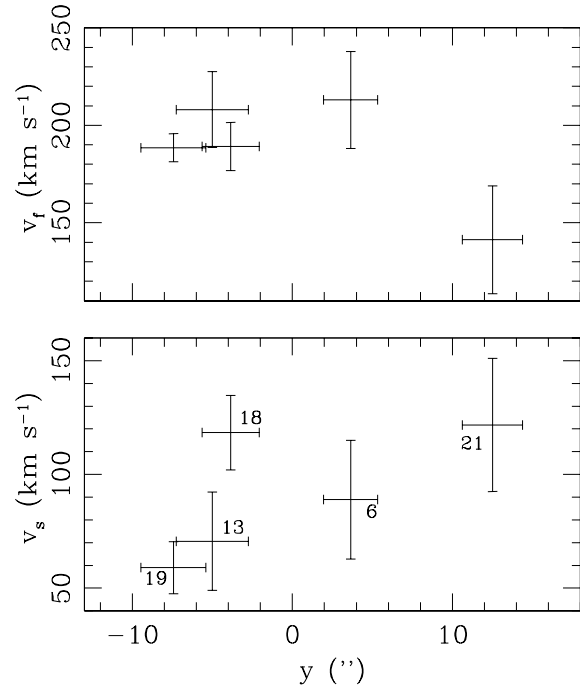


Fig. 2. Flow velocity ahead of HH 34S (top) and shock velocity (bottom) derived for the regions within the boxes shown in Fig. 1 (also see Reipurth et al. 2002). The horizontal bars give the location and size of the respective cross-correlation boxes (which are identified by the numbers beside each point on the bottom plot). The vertical bars give the errors in the derived velocities. These errors are dominated by the uncertainty in the orientation θ of the filaments, which was estimated to have a $\Delta\theta \approx 1^\circ$ value.

proper motions correspond to the real, material motion of the gas in the post-bowshock flow. For this to be the case, the observed knots of HH 34S should correspond to regions of enhanced emission which are advected within the post-bowshock flow, and remain visible during the ≈ 4 yr baseline of the *HST* images used for the proper motion determinations (see Reipurth et al. 2002). As was first pointed out by Raga & Böhm (1987), condensations with these properties do indeed appear in numerical simulations of bowshock flows, and these condensations remain visible for a time comparable to the cooling timescale of the post-bowshock flow (which is of the order of ~ 100 yr for typical parameters of HH bowshocks, see, e.g., Hartigan et al. 1987).

2. THE PROPER MOTIONS AND THE FLOW FIELD AHEAD OF HH 34S

In Figure 1 we show a schematic diagram with the filamentary structure seen in the $H\alpha$ *HST* images of HH 34S and the proper motions determined by

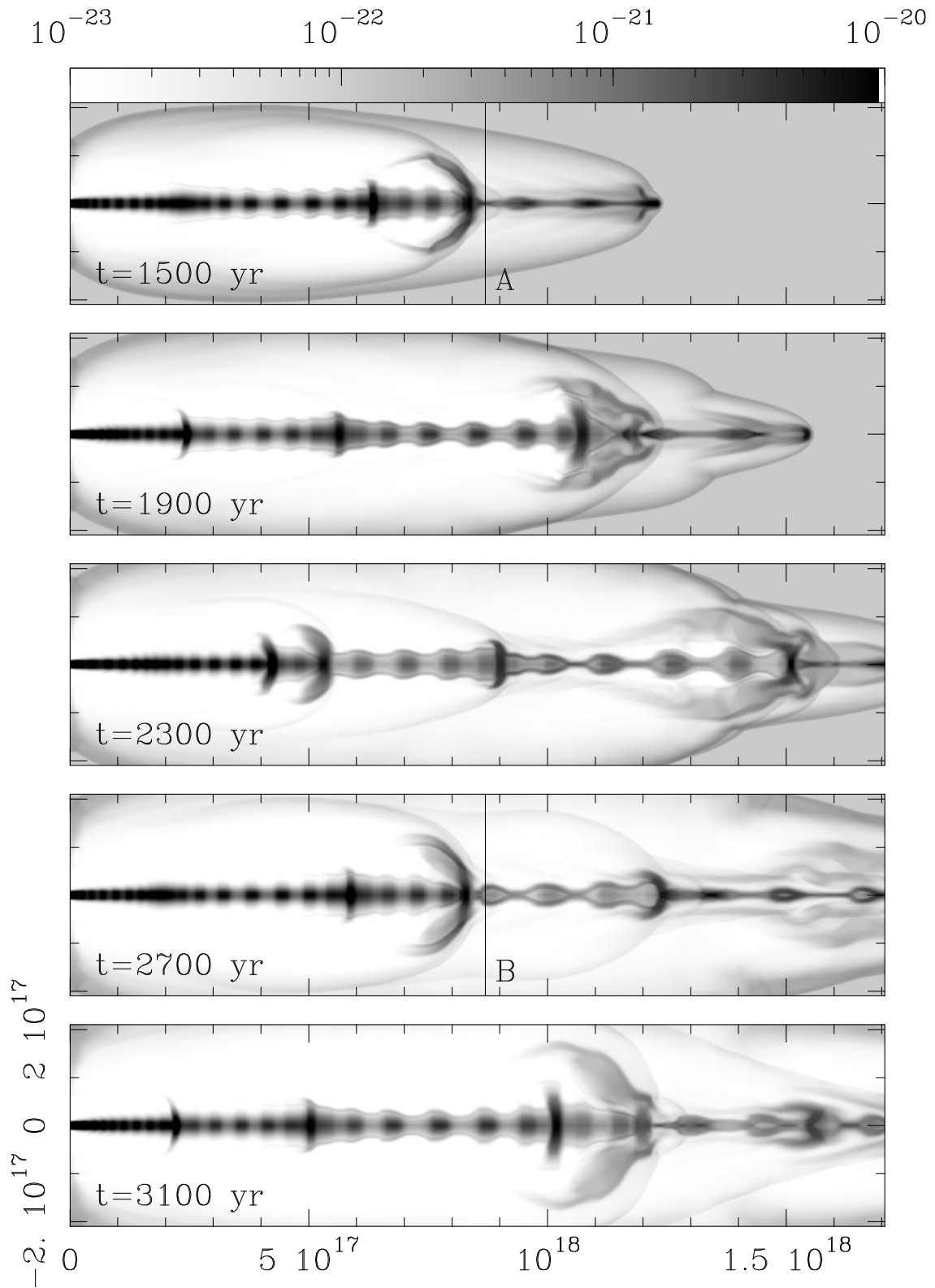


Fig. 3. Density stratifications predicted from the variable ejection velocity jet model described in § 3. The integration times are indicated on each plot. The stratifications are depicted with a logarithmic greyscale given (in g cm^{-3}) by the bar at the top of the graph. The axes are labeled in cm.

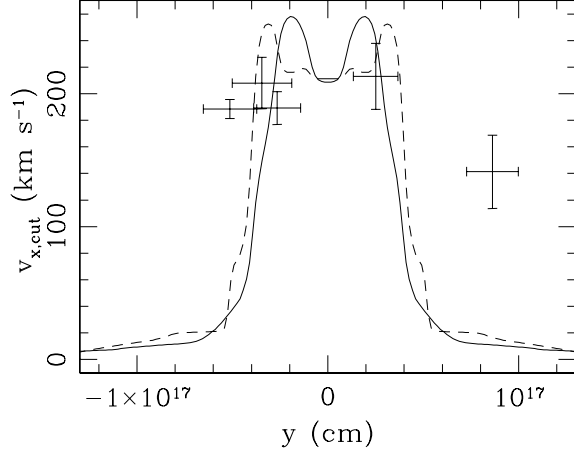


Fig. 4. Axial velocity cross sections through cuts A (solid line) and B (dashed line), at the positions shown in Fig. 3. The large crosses indicate the flow velocity v_f ahead of HH 34S derived from the proper motions of Reipurth et al. (2002), which are also shown in Fig. 2. In order to put these measurements together with the theoretical prediction, we have assumed a distance of 460 pc to HH 34.

Reipurth et al. (2002). The very detailed observed structures permit a new kind of analysis that was not previously possible.

Raga et al. (1997) derived simple expressions relating the observed proper motions to the velocity of the bowshock v_{bs} with respect to the surrounding medium, the orientation angle ϕ with respect to the plane of the sky, and the velocity v_f of the flow ahead of the bowshock. This velocity was assumed to have a single value (independent of position), and to be the result of the previous ejection history of the outflow source. Similar expressions relating the same flow parameters with the radial velocities observed in the emission line profiles had been previously derived by Hartigan et al. (1987).

We find that the very detailed proper motions measured by Reipurth et al. (2002) allow us to go further, relaxing the assumption of a position-independent v_f , and attempting to reconstruct the cross section of the flow velocity ahead of the HH 34S bowshock. This reconstruction is carried out as follows.

From Fig. 1, it is completely clear that the proper motions of condensations on the projected rim of the bowshock do not point in a direction normal to the bowshock surface. All of the proper motions point somewhere in between the shock normal and the outflow direction.

Because of the fact that a shock pushes material only in the direction of the shock normal, the com-

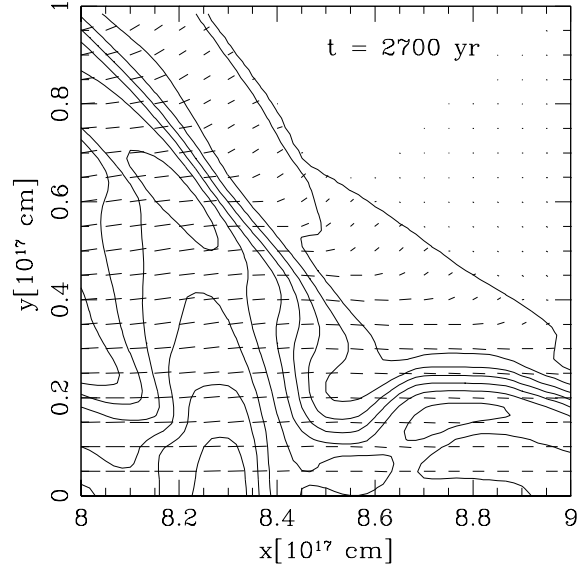


Fig. 5. Density stratification (solid lines, corresponding to factor of 2 contours) and flow velocities (line segments) in the region around the large working surface upstream of cut B (see Fig. 3). It is clear that the region ahead of the working surface has a flow velocity which is directed mostly along the symmetry axis. The x and y coordinates are the same as in Fig. 3, and can be used to locate the region shown in this graph within the full computational domain.

ponents of the proper motion velocities tangential to the shock surface ($v_{t,sky}$) have to be present in the pre-shock flow. The velocity $v_{t,sky}$ is related to the full velocity v_t tangential to the surface of the bowshock through the relation $v_{t,sky} = v_t \cos \phi$.

Therefore, the component along the plane of the sky of the tangential pre-bowshock velocity is $v_{t,sky} = v_x \cos \theta - |v_y| \sin \theta$, where v_x and v_y are the components of the proper motion velocity along and across the outflow axis, and θ is the angle between the outflow axis and the local direction of the surface of the bowshock ($\theta \geq 0$, see Fig. 1).

If we assume that the material ahead of the bowshock moves in a direction parallel to the outflow axis, we can then de-project $v_{t,sky}$ to obtain the full velocity of the pre-shock flow:

$$v_f = \frac{v_{t,sky}}{\cos \theta \cos \phi} = \frac{v_x - |v_y| \tan \theta}{\cos \phi}, \quad (1)$$

where ϕ is the angle between the outflow axis and the plane of the sky.

It is also then possible to compute the shock velocity as the difference between the components along the shock normal of the proper motion velocity and the velocity of the material directly ahead of

the bowshock:

$$v_s = v_x \sin \theta + |v_y| \cos \theta - v_f \sin \theta \cos \phi = |v_y| / \cos \theta. \quad (2)$$

To derive this equation, we have assumed that the difference between the pre- and post-shock normal velocities is equal to the shock velocity, which is approximately correct for large compression, radiative shocks.

Equations (1) and (2) can be used to determine the shock velocity and the velocity of the material ahead of the bowshock for all of the filamentary condensations along the leading edge of the bowshock. In this way, the assumption of a position-independent v_f (which was made by Hartigan et al. 1987 and Raga et al. 1997) can now be relaxed.

Reipurth et al. (2002) have measured proper motions along and across the axis of HH 34S using a series of cross-correlation boxes. For our analysis, we have chosen the boxes on the bowshock rim, and only the ones within which filamentary structures with well defined orientations are observed. With these two criteria, we have selected boxes 19, 13, 18, 6, and 21 of Reipurth et al. (2002, also see Fig. 1). For the filaments within each of these boxes, we have measured the orientation between the direction of the filament and the outflow axis (the angle θ of Fig. 1) and taken the corresponding proper motions measured by Reipurth et al. (2002). We have chosen the $\phi = 30^\circ$ angle between the outflow axis and the plane of the sky determined by Heathcote & Reipurth (1992).

The results obtained from equations (1) and (2) for the five chosen cross correlation boxes are shown (as a function of distance from the outflow axis) in Figure 2. This figure shows that even though the errors are rather large, it is possible to reconstruct the profiles of the shock velocity v_s and the downstream flow velocity v_f along the leading edge of HH 34S. We find that the shock velocities range from 60 to 120 km s⁻¹, which is in principle consistent with the high excitation nature of the object (see, e.g., Bührke, Mundt, & Ray 1988).

We believe that this is the first ever determination of the shock velocities of an HH object purely from kinematic data. The fact that it gives velocities that are in the correct range, as deduced from comparisons of observed line ratios with predictions from plane-parallel shock models (see, e.g., Raymond 1979; Hartigan et al. 1987; Raga, Böhm, & Cantó 1996), is reassuring.

Interestingly, we find that the flow velocity v_f ahead of HH 34S has values ranging from 140 up to 215 km s⁻¹, with the higher velocities close to

the symmetry axis, and lower velocities farther away along the bowshock wings (see Fig. 2). If we take this result at face value, it implies that HH 34S is moving into a region which is moving away from the outflow source with a velocity of ~ 200 km s⁻¹. As is clear from Fig. 2, this high velocity flow extends to $\sim 10''$ to each side of the outflow axis, and has a strongly decreasing velocity for larger distances from the axis.

The nature of the flow ahead of HH 34S is not completely clear. Two explanations are possible:

1. HH 34S could be moving into a very wide, high velocity wake left behind by previous outflow events,
2. the high velocity material ahead of HH 34S could be associated with a broader outflow (ejected from the same source) within which is travelling the optically observed HH 34 jet. The existence of such broad outflows ejected from young stars has been frequently suggested in the literature.

Clearly, both possibilities are intriguing, and deserve further study. However, we concentrate on the first of these two scenarios, and investigate it further in the following section.

3. HH 34S MOVING INTO THE WAKE OF PREVIOUS OUTFLOW EVENTS

It has long been suggested that the structure of knots along the HH 34 jet could be the result of a time-variability of the outflow source (e.g., Raga et al. 1990; Reipurth & Heathcote 1992). More recently, it has been found that HH 34S is not the first outflow event, but that it is moving behind a series of previous bowshocks (Bally & Devine 1994; Devine et al. 1997). Therefore, it is in principle not unreasonable to consider whether the velocity cross section of the material ahead of HH 34S corresponds to the wake left behind by the previous outflow episodes.

In order to study this possibility, we consider the 3-mode velocity time-variability proposed by Raga & Noriega-Crespo (1998) for modelling the knot structure of the HH 34 jet. These authors considered a jet with an ejection velocity with a mean velocity of 280 km s⁻¹, and three sinusoidal modes of half-amplitudes of 70, 15 and 40 km s⁻¹ with periods of 1200, 27, and 310 yr (respectively).

We have re-calculated an axisymmetric jet model with this time-dependent ejection velocity. We have also assumed that the jet has a top-hat initial

cross section of radius $r_j = 10^{16}$ cm, and a time-independent injection number density of 5000 cm^{-3} . The jet travels into a homogeneous environment with a number density of 50 cm^{-3} and a temperature of 1000 K. Both the jet and the environment are assumed to be initially neutral (except for Carbon, which is singly ionized).

The present simulation was carried out including the same ions, atomic parameters and radiative cooling as in Raga & Noriega-Crespo (1998), but was computed with an axisymmetric version of the yguazú-a code. This code uses the flux vector splitting algorithm of van Leer (1982), implemented on a binary adaptive grid, and is described in detail by Raga et al. (2000). A 4-level grid with a maximum resolution of 1.64×10^{15} cm (along both the axial and radial directions) was used.

The results obtained from this simulation are illustrated in Figure 3, which shows the resultant density cross section time sequence. From the fact that the deprojected distance from the head of HH 34S to the outflow source is $x_{\text{HH34S}} \approx 8.8 \times 10^{17}$ cm, we see that two of the time frames of Fig. 3 (the $t = 1500$ and 2700 frames) do have a major working surface at the correct position. For these two time-frames, we have extracted an axial velocity versus position $v_x(y)$ cut immediately ahead of these working surfaces. These cuts have been taken through the lines A and B (corresponding to the $t = 1500$ and the $t = 2700$ yr frames, respectively) shown in Fig. 3.

The axial velocity cross sections immediately ahead of the working surfaces obtained from cuts A and B are shown in Figure 4. The corresponding $v_x(y)$ profile obtained from the HH 34S observations of Reipurth et al. (2002, also see § 2) is superimposed on the predictions from the numerical simulations. It is clear that there is good qualitative agreement between the models and the observations for both the velocity magnitude and the spatial scale (perpendicular to the symmetry axis).

The one exception is that the velocity ahead of the bowshock in the region of box 21 (see Fig. 1 and Reipurth et al. 2002) appears to differ significantly from the model predictions. As can be seen even in early images of HH 34 jet (see the discovery paper of Reipurth et al. 1986), the two wings of HH 34S are not symmetric. The rather strong observed asymmetry might be a result of the precession of the outflow direction, which is apparent in the parsec scale structure of the outflow (Devine et al. 1997) or might be due to inhomogeneities present in the environment.

Clearly, in the context of our present, axisymmetric calculations, such asymmetries cannot be mod-

eled. Because of this, it is not clear whether or not the flow velocity deduced from the proper motion of box 21 (see Figs. 1 and 4) is a real discrepancy between the observations and a “wake” interpretation for the velocity cross section ahead of HH 34S.

Finally, in Figure 5 we show the velocity field in the region around cut B (see the $t = 2700$ yr frame of Fig. 3). From this figure, it is clear that ahead of the working surface, the flow velocity is quite closely parallel to the symmetry axis out to a radius of $\sim 4 \times 10^{16}$ cm. This result shows that the assumption that the flow ahead of HH 34S is parallel to the symmetry axis (made in § 2) appears to be correct, at least in the case in which this velocity is due to the passage of previous working surfaces of the outflow.

4. CONCLUSIONS

We have analyzed the HST proper motions of HH 34S of Reipurth et al. (2002). These authors measured the proper motions of many filaments with well defined directions, and these can be used to derive the velocities parallel and perpendicular to the shocks.

Using the fact that in a radiative shock the normal velocity (measured in a coordinate system fixed to the shock) is basically eliminated, and the tangential velocity is preserved, one can reconstruct the flow field ahead of the HH 34S bowshock. Also, the shock velocity (as a function of position along the HH 34S wings) can be derived.

The derivation of the flow field ahead of the bowshock is based on the assumption that no mixing occurs between the observed region of the post-bowshock flow and the jet material. If such mixing were to occur, part of the observed motion tangential to the shock could be generated locally, and this motion would therefore not directly reflect the flow velocity of the material ahead of the bowshock.

From these simple considerations, we derive shock velocities for HH 34S in the 60 to 120 km s^{-1} range. Reassuringly, these shock velocities are consistent with previous estimates based on line ratios and/or line profiles (see, e.g., Morse et al. 1992).

For the flow velocity ahead of HH 34S, we find values of $\approx 200 \text{ km s}^{-1}$. The region which is in motion is quite wide, extending out to $\sim 10''$ away from the outflow axis. The existence of this broad flow ahead of HH 34S is quite intriguing, and to some extent resembles the broad emitting region detected around the HH 111 jet in the spectroscopic observations of Riera et al. (2001).

In order to see if the motion ahead of HH 34S is consistent with a collimated jet model, we have re-computed the variable ejection velocity HH 34 jet model of Raga & Noriega-Crespo (1998). From the resulting flow, we have calculated the velocity cross section ahead of working surfaces located at the distance (from the source) of HH 34S. We find that the predicted velocity cross sections are in good agreement with our determination of the flow velocity ahead of HH 34S.

From this comparison, we see that a variable ejection velocity jet automatically produces a quite broad, moving envelope (corresponding to the wakes of previous outflow events), which has kinematical properties that resemble the flow ahead of HH 34S. Because of this, we feel that at the present time it is not reasonable to interpret the flow ahead of HH 34S as evidence for a “broad wind” ejected from the outflow source.

This research was supported by the CONACyT grants 34566-E and 36572-E. AR acknowledges support from a fellowship of the John Simon Guggenheim Memorial Foundation. PFV is a fellow of CONICET. We acknowledge Israel Díaz for his help in setting up the new computer with which the present calculations were carried out.

REFERENCES

- Bally, J., & Devine, D. 1994, *ApJ*, 428, L65
 Bührke, T., Mundt, R., & Ray, T. P. 1988, *A&A*, 200, 99
 Curiel, S., Raga, A. C., Raymond, J. C., Noriega-Crespo, A., & Cantó, J. 1997, *AJ*, 114, 2736
 Devine, D., Bally, J., Reipurth, B., & Heathcote, S. 1997, *AJ*, 114, 2095
 Eisloffel, J., & Mundt, R. 1992, *A&A*, 263, 292
 Hartigan, P., Morse, J. A., Reipurth, B., Heathcote, S., & Bally, J. 2001, *ApJ*, 559, L157
 Hartigan, P., Raymond, J. C., & Hartmann, L. 1987, *ApJ*, 316, 323
 Heathcote, S., & Reipurth, B. 1992, *AJ*, 104, 2193
 Morse, J. A., Hartigan, P., Cecil, G., Raymond, J. C., & Heathcote, S. 1992, *ApJ*, 399, 231
 Raga, A. C., & Böhm, K. H. 1987, *ApJ*, 323, 193
 Raga, A. C., Böhm, K. H., & Cantó, J. 1996, *RevMexAA*, 32, 161
 Raga, A. C., Cantó, J., Binette, L., & Calvet, N. 1990, *ApJ*, 364, 601
 Raga, A. C., Cantó, J., Curiel, S., Noriega-Crespo, A., & Raymond, J. C. 1997, *RevMexAA*, 33, 157
 Raga, A. C., Navarro-González, R., & Villagrán-Muniz, M. 2000, *RevMexAA*, 36, 67
 Raga, A. C., & Noriega-Crespo, A. 1988, *AJ*, 116, 2943
 Raymond, J. C. 1979, *ApJS*, 39, 1
 Reipurth, B., Bally, J., Graham, J. A., Lane, A. P., & Zealy, W. J. 1986, *A&A*, 164, 51
 Reipurth, B., & Heathcote, S. 1992, *A&A*, 257, 693
 Reipurth, B., Heathcote, S., Morse, J., Hartigan, P., & Bally, J. 2002, *AJ*, 123, 362
 Riera, A., López, R., Raga, A. C., Anglada, G., & Estalella, R. 2001, *RevMexAA*, 37, 147
 van Leer, B. 1982, ICASE Report No. 82-30.

Jorge Cantó and Elena Masciadri: Instituto de Astronomía, UNAM, Apartado Postal 70-264, 04510 México D. F., México.

Alejandro C. Raga and Pablo F. Velázquez: Instituto de Ciencias Nucleares, UNAM, Apartado Postal 70-543, 04510 México, D. F., México (raga@astroscu.unam.mx).